the single-scattering approximation made with the earlier data.

ACKNOWLEDGMENTS

The authors would like to thank Dr. K. K. Young, Dr. K. Ruddick, and R. H. Ball for their assistance during parts of the run. The aid of the Brookhaven cosmotron staff in setting up and running the experiment is much appreciated. We take this opportunity to thank Professor L. W. Jones for several useful discussions.

PHYSICAL REVIEW VOLUME 164, NUMBER 5 25 DECEMBER 1967

Measurement of $\pi^- p$ Elastic Scattering at 180°*

S. W. KORMANYOS,† A. D. KRISCH, J. R. O'FALLON,‡ AND K. RUDDICK§
The Randall Laboratory of Physics, The University of Michigan, Ann Arbor, Michigan

AND

L. G. RATNER
Particle Accelerator Division, Argonne National Laboratory, Argonne Illinois

(Received 21 July 1967)

We have measured the differential cross section for $\pi^- p$ elastic scattering at 180° in steps of 0.10 GeV/c or less in the region $P_0=1.6$ to 5.3 GeV/c. We detected elastic scattering events, from protons in a liquid H_2 target, with a double spectrometer consisting of magnets and scintillation counters in coincidence. The incident π^- beam was counted by scintillation counters. The cross section was found to have considerable structure. This may be interpreted as interference between the resonant amplitudes and the nonresonant or background amplitude. Very strong destructive interference occurs around $P_0=2.15$ GeV/c, where the cross section drops almost two orders of magnitude in passing through the $N^*(2190)$. Another interesting feature of the data is a large narrow peak in the cross section at $P_0=5.12$ GeV/c, providing firm evidence for the existence of a nucleon resonance with a mass of 3245±10 MeV. This $N^*(3245)$ has a full width of less than 35 MeV, which is about 1% of its mass. From this experiment we were able to determine the parity and the quantity $\chi(J+\frac{1}{2})$ for each N^* resonance, where χ is the elasticity and J is the spin of the resonance.

1. INTRODUCTION

IN recent years many high-energy physics experiments have investigated the existence and properties of resonances. Traditionally the mass, width, and isotopic spin have been studied in total-cross-section measurements. These resonances caused structure in total cross sections from which certain properties of the resonances could be deduced. The spins and parities have traditionally been determined from angular distributions in elastic scattering.

In this experiment a different technique was employed to study the properties of resonances. We measured a differential elastic cross section at 180° as a function of energy. Because of the interference of the resonances with the background, quite a bit of structure was present in the cross section. From the data we were able to determine the parity and the quantity $\chi(J+\frac{1}{2})$ for various N^* resonances. This method of studying resonances appears to be more sensitive than studying the total cross section.

We have measured[1,2] the differential cross section for $\pi^- p$ elastic scattering at 180° in steps of 0.10 GeV/c or less in the region $P_0=1.6$ to 5.3 GeV/c. This experiment was done at the zero-gradient synchrotron ZGS at Argonne National Laboratory. The differential cross section for $\pi^- p$ elastic scattering in the backward hemisphere has been measured in other experiments.[3–9] However, essentially none of them have taken measurements as far back as 180°.

There is considerable structure in the cross section.

* Work performed under the auspices of the U. S. Atomic Energy Commission and the Office of Naval Research.

† Present address: Bendix Aerospace Systems Division, Ann Arbor, Michigan.

‡ Present address: Department of Physics, Saint Louis University, Saint Louis, Missouri.

§ Present address: Department of Physics, University of Minnesota, Minneapolis, Minnesota.

[1] S. W. Kormanyos, A. D. Krisch, J. R. O'Fallon, K. Ruddick, and L. G. Ratner, Phys. Rev. Letters **16**, 709 (1966).

[2] For further details see S. W. Kormanyos' thesis, University of Michigan, 1966 (unpublished).

[3] W. R. Frisken, A. L. Read, H. Ruderman, A. D. Krisch, J. Orear, R. Rubinstein, D. B. Scarl, and D. H. White, Phys. Rev. Letters **15**, 313 (1965); Phys. Rev. **152**, 1162 (1966).

[4] P. J. Duke, D. P. Jones, M. A. R. Kemp, P. G. Murphy, J. D. Prentice, J. J. Thresher, H. H. Atkinson, C. R. Cox, and K. S. Heard, Phys. Rev. Letters **15**, 468 (1965); and (private communication).

[5] C. T. Coffin, N. Dikmen, L. Ettlinger, D. Meyer, A. Saulys, K. Terwilliger, and D. Williams, Phys. Rev. Letters **15**, 838 (1965).

[6] D. E. Damouth, L. W. Jones, and M. L. Perl, Phys. Rev. Letters **11**, 287 (1963).

[7] W. F. Baker, P. J. Carlson, V. Chabaud, A. Lundby, E. G. Michaelis, J. Banaigs, J. Berger, C. Bonnel, J. Duflo, L. Goldzahl, and F. Plouin, Phys. Letters **23**, 605 (1966).

[8] M. L. Perl, Y. Y. Lee, and E. Marquit, Phys. Rev. **138**, B707 (1965).

[9] J. A. Helland, C. D. Wood, T. J. Devlin, D. E. Hagge, M. J. Longo, B. J. Moyer, and V. Perez-Mendez, Phys. Rev. **134**, B1079 (1964).

This may be interpreted as an interference effect between the resonant amplitude and the nonresonant or background amplitude. There is a dramatic destructive interference at $P_0=2.15$ GeV/c which is quite interesting as the cross section drops almost two orders of magnitude in this region. We also observed a large narrow peak in the cross section at $P_0=5.12$ GeV/c. We believe that this is a clear indication for a nucleon resonance with a mass of 3245±10 MeV. The width of this resonance is less than 1% of its mass. It seems remarkable that such a massive particle should be so stable.

Assuming a smooth background amplitude, the parities of various N^* resonances were determined. We also calculated the quantity $\chi(J+\frac{1}{2})$ for these resonances where χ is the elasticity and J is the spin of the resonance.

2. EXPERIMENTAL TECHNIQUE

Our system employed a double spectrometer to detect elastic scattering events. Each spectrometer consisted of a bending magnet for momentum analysis and a telescope of scintillation counters for detection. The target protons were contained in a liquid hydrogen target and the incident π^- beam was counted with scintillation counters.

A. Circulating Proton Beam

Figure 1 shows the beam layout. The 12.5-GeV/c circulating proton beam of the AGS struck an internal popup target $\frac{1}{8}\times\frac{1}{8}\times3.85$ in. long. This target contained 90% copper and 10% aluminum and had a thin beryllium lip. During the acceleration cycle, the target was out of the beam. After completion of the acceleration cycle, the target was moved up and the beam was brought onto the target. The circulating proton beam made many passes through this internal target during the spill time of approximately 150 msec. The repetition rate was about 2.5 sec and the ZGS beam intensity was about 5×10^{11} protons per pulse.

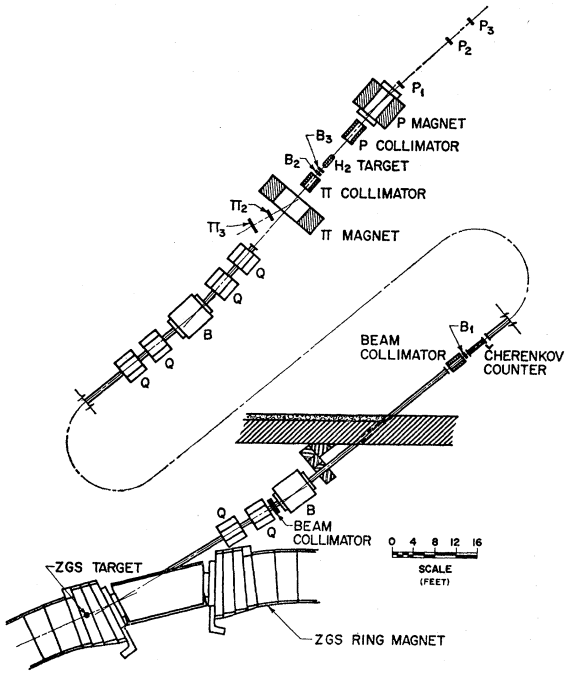

FIG. 1. Experimental layout. The ZGS ring, the 17° beam, and our double spectrometer are shown.

The internal target was placed at various positions from 3 to 5 ft back into the field of the ZGS ring magnet. The ring magnet deflected the negative pions, produced at small angles, through the angle necessary to send them down the 17° beam line. The pion production angle was chosen as close to zero degrees as possible in order to yield maximum production. The appropriate internal target coordinates were calculated before the run. At each new pion energy the internal target was moved to the correct position and angle with a remote drive mechanism.

B. π Beam

The π^- beam intensity was about 3.5×10^5 pions per 5×10^{11} circulating protons in the region 2.0 to 4.0 GeV/c.[10] At higher and lower momenta the intensity dropped off. At lower momenta more beam pions decayed, while at higher momenta the pion production cross section decreased. Throughout most of the experiment the beam intensity was in the range of 1×10^5 to 3.5×10^5 pions per pulse.

The pion beam line is shown in Fig. 1. It consisted of three quadrapole doublets for focusing and two bending magnets for momentum analysis. There was an intermediate focus at the second beam collimator and a second focus at the liquid hydrogen target. The beam had a momentum bite of $\Delta P/P=\pm\frac{3}{4}\%$ and subtended a solid angle of 1×10^{-4} sr at the internal ZGS target. This gave beam particles with angular divergences of less than ±3 mrad at the target.

The beam bending magnets were 18 in. wide, 6 in. high, and 72 in. long. The quadrapole magnets had 10-in. nominal diameters and were 36 in. long. To define the solid angle there was a beam collimator between the second quadrapole and the first bending magnet, which was 3.5 in. wide, 4.5 in. high, and 24 in. long. There was a 1-in. by 1-in. collimator at the first focus, which defined the momentum of the beam. The pion beam also passed through the π magnet which has to be adjusted so that the beam passed through the center of the H_2 target.

At each new incident beam energy the beam was retuned. A beam monitor consisting of three small scintillation counters was placed near Q_1 inside the ZGS ring shielding. The triplet coincidence rate of these counters ($M=M_1M_2M_3$) was directly proportional to

[10] L. G. Ratner, Argonne National Laboratory internal report (unpublished).

the ZGS flux. Tuning consisted of maximizing the number of beam pions relative to this monitor.

In changing to a different energy the internal target was moved to a new position. The quadrapoles and bending magnets were set at their calculated values. Then the beam was tuned as follows. First B_1 was tuned, then Q_1, Q_2, Q_6, Q_7, Q_5, and Q_8; finally B_1 was rechecked. Typical tuning curves are shown in Fig. 2. B_2 was not tuned but was set and held at its calculated value. The rest of the beam was tuned around B_2. We calibrated the magnetic field of B_2 as a function of magnet current with nuclear-magnetic-resonance techniques over the entire range of the experiment. Hysteresis effects were found to be well below 1%. Using this calibration the laboratory momentum of the pion beam was known to ± 0.03 GeV/c. The magnet currents were set during the experiment by using digital voltmeters to read the voltage across a precision shunt in series with the magnets.

The beam pions were counted by the scintillation counters B_1, B_2, and B_3 in coincidence with a gas threshold Čerenkov counter containing 80–140 psi of ethane. This beam coincidence was referred to as BC. The Čerenkov counter discriminated against antiprotons and K mesons which comprised less than 1% of the beam. As the beam energy was increased we decreased the Čerenkov pressure so that we would still discriminate against kaons. The first beam counter B_1 was a 1-in.-square, $\frac{1}{8}$-in.-thick counter, placed at the first focus. The B_2 and B_3 counters were 1-in.-diam disks $\frac{1}{8}$ in. thick and were placed immediately in front of the hydrogen target. The B_2 and B_3 counters pointed in opposite directions with only the scintillators overlapping so that the pions had to go through both scintillators in order to be counted. Had the counters pointed in the same direction, pions could have gone through both light pipes, given off Čerenkov light, been counted as a beam pion, and yet missed the hydrogen target.

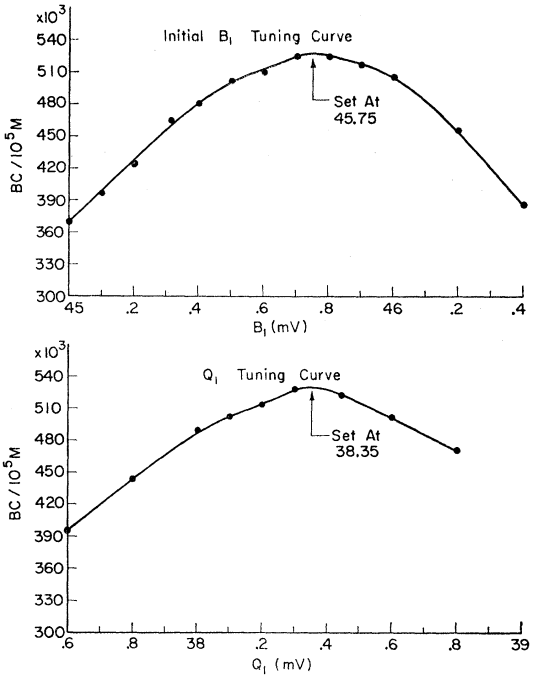

FIG. 2. Beam tuning curves showing the ratio of beam pions to monitor counts as the B_1 and the Q_1 magnets are varied.

C. Hydrogen Target

The source of the target protons was a liquid hydrogen target. This cylindrical target was 12 in. long and $1\frac{1}{2}$ in. in diameter with its axis along the beam axis. During the course of the experiment the target was moved and surveyed into a new position twice, so that the scattered pions would not have to be bent through too large an angle. Thus there were three beam "geometries" in the experiment as shown in Fig. 3.

The liquid H_2 target was $1\frac{1}{2}$ in. in diameter. However, the interaction region was defined by the 1-in.-diam circular beam counters (B_2,B_3). This arrangement insured that the detected incident beam particles did indeed pass through the hydrogen in the target. Events caused by beam pions which did not pass through B_2 and B_3 were exlcuded from our detection system electronically.

D. Detection System

The detection system for the scattered particles was comprised of a double spectrometer, in coincidence. Each spectrometer consisted of a bending magnet for momentum analysis (π magnet or p magnet) and a telescope of scintillation counters to detect the scattered particles ($\pi = \pi_2\pi_3$ or $p = p_1p_2p_3$). The experimental layout is shown in Figs. 1 and 3.

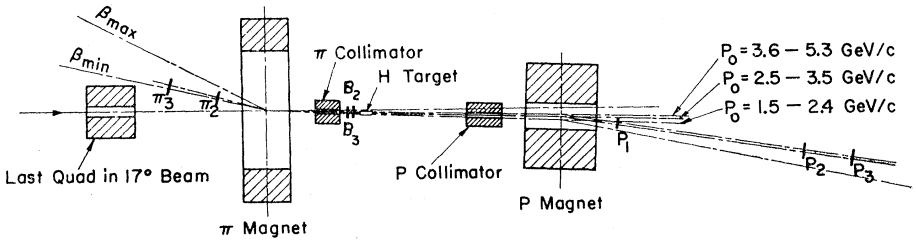

FIG. 3. Experimental layout showing the double spectrometer in detail. The three different "geometries" used in the different energy ranges are shown.

The incident π passed through the π magnet and was bent through a small angle. It then passed through the B_2 and B_3 beam counters and into the hydrogen target. After a 180° scattering the backward scattered π passed through the π magnet in the opposite direction to the beam and was deflected so that it passed through the π telescope (π_2 and π_3). Thus the scattered π was cleanly separated from the incident π beam. The forward scattered proton passed through the p magnet which deflected it into the p telescope (p_1, p_2, and p_3). The pions in the beam, which did not interact, were bent in the opposite direction because they had the opposite electrical charge to the protons. In this way the scattered protons were also cleanly separated from the noninteracting π^- beam.

The incident and scattered pions passed through the π collimator while the scattered protons passed through the p collimator. These collimators were considerably oversized so that the scintillation counters rather than the collimators defined the solid angle.

The current settings in the π and p magnets and the counter telescope angles were determined as follows. For a given geometry and incident momentum, we calculated the π-magnet field integral needed to bring the incident π beam onto the hydrogen target. Once the field integral was set the angle of the π telescope was defined since the momentum of the backscattered π^- was determined by kinematics. Finally the magnetic field of the p magnet was adjusted so that the forward-scattered proton would be bent into the proton telescope.

The p magnet was a standard bending magnet 72 in. long with a 6-in. by 18-in. gap. The π magnet was a large gap bending magnet 30 in. long, 14 in. high, and 84 in. wide. The momentum bite of the π telescope was about $\Delta P/P = \pm 30\%$, while for the p telescope $\Delta P/P$ was about $\pm 10\%$.

The center-of-mass solid angle was defined by the 16.-in×16-in. π_3 counter which was 200 in. from the hydrogen target. It varied between 1.5 and 0.5 msr during the course of the experiment. The p_3 counter (9in.×9 in.) was 500 in. from the target and was overmatched to subtend a somewhat larger solid angle in the center-of-mass system. The overmatching allowed for such things as the momentum spread and angular divergence of the incident beam, a 1% variation of the magnetic field of the p magnet, a 3% variation of the magnetic field of the π magnet, the H_2 target size, and the multiple Coulomb scattering of both scattered particles. By overmatching the proton counters in this way, in scattering was made equal to out scattering and no correction to the raw data was necessary. The various terms making up the overmatching were assumed to be independent and were combined in quadrature. This overmatching represented about one standard deviation. At most energies there were at least two standard deviations of overmatching.

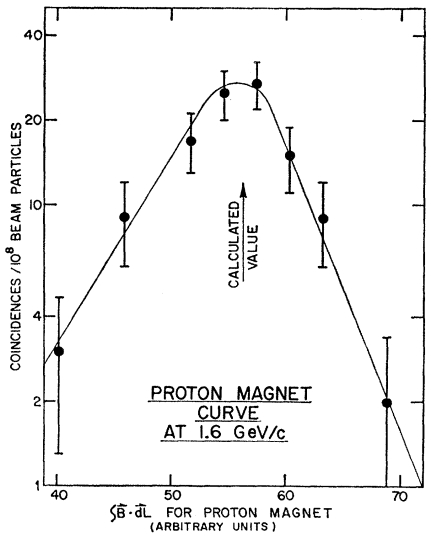

FIG. 4. Proton bending magnet curve showing the number πp coincidences as a function of magnet current.

At 1.6 GeV/c we ran a p-magnet curve. This consisted of measuring the ratio of event rate to beam intensity while varying the magnetic field in the p magnet. See Fig. 4. This ratio reached a peak at the calculated value of the magnetic field integral and decreased on both sides. This showed that all magnets were correctly calibrated and that there were no surveying errors. This was also evidence that we were indeed observing elastic scattering.

An important advantage of the experimental technique used was that in changing from one measurement to the next only two counters were moved. The current in the π magnet was increased so that the higher-momentum incident beam still passed through the hydrogen target. The current in the p magnet was increased so that the higher-momentum protons still passed through the p telescope. The only physical change was moving the π telescope by about 1°. This consisted of moving the two π counters by about 1 in. We also made small timing changes to compensate for the changes in time of flight of the π and p. By not moving the hydrogen target, the magnets, or the p counters, we removed the possibility of systematic errors due to misalignment.

E. Counters and Electronics

The counters consisted of $\frac{1}{2}$-in.-thick sheets of Pilot B scintillator with tapered Lucite light pipes. Both the scintillator and light pipe were wrapped with aluminum foil and black masking tape to give internal reflection without light leaks. The counters were about 1 ft by 1 ft in size and they were optically connected to RCA 7746 photomultiplier tubes by Lucite light pipes. The photomultipliers were fast 10 stage tubes; the time between the light pulse and the voltage pulse was stable to less than 1 nsec. The pulse rise time itself was about 2 nsec,

but by triggering on the rising edge of the voltage pulse a stability of better than 1 nsec was achieved.

The pulses from the phototubes were carried by 50 Ω RG 213/U cables to the electronic logic system. Within the electronic logic system the signals were carried by 50 Ω RG 223/U double shielded cables. The signal cables were cut to specified lengths; the pulse transit time was calculated and independently measured for each cable using reflected pulses, generated by a fast pulser. The time delays of the electronics logic system were first calculated, and then checked with the pulser. The timing was further checked by running delay curves at 1.6 GeV/c where the counting rate was high. The high voltage on the tubes was supplied by 3kV power supplys via a distribution panel and read on two Cimron 4-place digital voltmeters in parallel.

The logic system consisted of 100-Mc Chronetics coincidence circuitry. A block diagram of the logic system is shown in Fig. 5. The outputs of the logic system were displayed on 100-Mc, TSI 1535 scalers and recorded with a Polaroid camera. The 400-channel pulse-height analyzer was a TMC model 404 C. Important quantities were double scaled. The two signals from the π counters, π_2 and π_3, came together to form a twofold π coincidence. Similarly, the three p signals, p_1, p_2, and p_3, formed a threefold p coincidence. The resolving times were about 5 nsec. The p signal then formed a coincidence with the beam coincidence ($BC = B_1B_2B_3C$), denoted by pBC. Including the BC signal in the event coincidence ensured that only beam particles counted by B_2B_3 could result in events. The π and pBC signals were fed into the πp_{fast} coincidence circuit. If they arrived simultaneously within the 5-nsec resolving time, they formed a πp_{fast} coincidence. The number of πp_{fast} coincidences would be equal to the number of elastic scattering events if there were no accidental events.

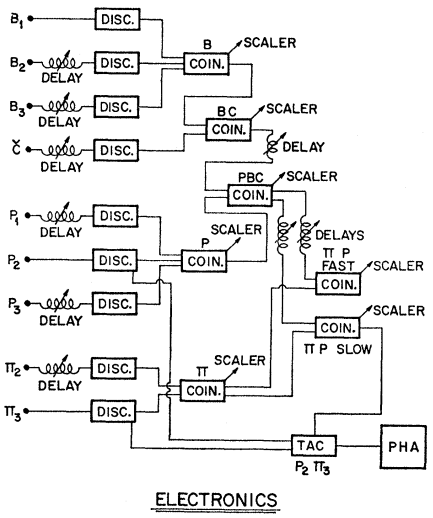

FIG. 5. Electronics block diagram for slow and fast coincidences and for time-of-flight analysis.

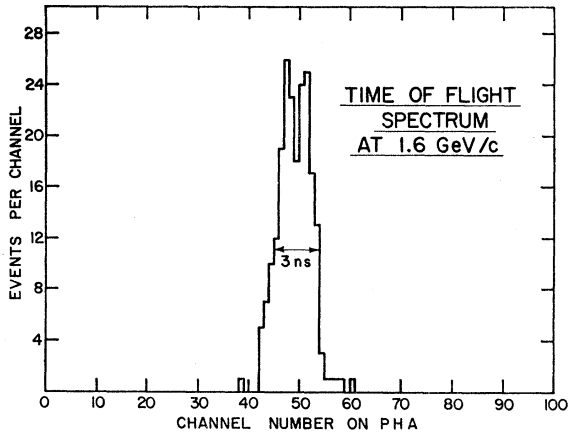

FIG. 6. Time-of-flight spectrum from the pulse-height analyzer. Number of coincidences is plotted against the time-of-flight difference between the scattered pion and proton.

Two techniques were used to estimate the number of accidental coincidences. The first employed the πp_{slow} coincidence circuit, which had a 30-nsec resolving time, in contrast to the 5-nsec resolving time of πp_{fast}. If the number of πp_{slow} coincidences was equal to the number of πp_{fast} coincidences, this indicated that there were no accidentals and all coincidences were true events. If πp_{slow} was greater than πp_{fast}, then the quantity ($\pi p_{\text{slow}} - \pi p_{\text{fast}}$) was some measure of the accidentals, assuming the two resolving times were well known.

The second, more reliable technique, used a time-to-amplitude converter (TAC) and a pulse-height analyzer (PHA). Each πp_{slow} coincidence triggered the TAC. Stretched pulses from p_2 and π_3 were fed into the TAC which gave out a pulse whose height in volts was proportional to the time overlap of the p_2 and π_3 pulses. This was then fed into the PHA which sorted the pulses into bins according to pulse height and then stored and displayed the number of pulses in each bin. Thus the PHA gave a display of the number of events versus the time-of-flight difference between the pion and proton. Such a time-of-flight spectrum is shown in Fig. 6. Each channel is about $\frac{1}{3}$ nsec. wide. The true events appeared as a large peak about 3 nsec wide, at half-maximum. 2 nsec of this was caused by the fact that the hydrogen target was 1 ft long. The accidentals would have appeared as a broad flat region about 30 nsec wide, which could be subtracted from the peak. The accidental subtraction was always less than one percent.

F. Background

There were two possible sources of background which might have simulated $\pi^- p$ elastic scattering at 180°. One possibility was accidental coincidences between the π and p telescopes. This was discussed in Sec. 2E where a 1% upper limit on accidental events was set. The other source was inelastic events.

It was necessary to show that our detection system

was not sensitive to inelastic pion-proton scattering events. The process most likely to mimic an elastic event was π^0 production,

$$\pi^-+p\rightarrow\pi^-+p+\pi^0. \quad (1)$$

The possibility of detecting events of this type was studied by taking carbon runs. These consisted of data runs taken with the hydrogen target emptied of hydrogen and a 2.5-in.-long carbon target placed just behind the empty hydrogen target flask. To see how these runs yield information on inelastic events, consider the following argument.

Suppose the constraints on angle and momentum were sufficiently lax that with the hydrogen target we were observing π^-p events that were in fact smeared by π^0 production. Then the additional smearing of angle and momentum introduced by the Fermi momentum of the protons in the carbon nucleus would not remove the counting rate. If, however, the kinematic constraints were sufficiently tight that the smear of the Fermi momentum removed most of the event rate, then we have evidence that π^0 production smears things too much to be detected significantly by the double spectrometer. This is true because the π^0 production introduces a greater smear than the Fermi momentum for any reasonable distribution of π^0 mesons. We took runs with a carbon target at 2.8 and 4.1 GeV/c and obtained two events. In equivalent runs with an H_2 target, over a hundred events were obtained. This is conclusive evidence for a 1% upper limit on inelastic contamination.

These carbon runs also showed that there were no accidental events, by the following argument. With the carbon target in place of the hydrogen target, the number of coincidences in the π telescope remained about the same, but the number of pBC coincidences increased by about a factor of two. Therefore, if we were counting accidental events we should have seen more with the carbon target. However, only two events were seen compared to over 100 with the hydrogen target. Thus we conclude that there were essentially no accidental events. The carbon runs simultaneously served as empty target runs since the carbon target was placed just behind the empty hydrogen target.

The reason for the small background lay in the tight kinematic constraints. The solid angle was 10^{-3} sr in the center-of-mass system, and the momentum bite of the proton spectrometer was $\pm10\%$ while the pion spectrometer had $\Delta p/p=\pm30\%$. Moreover, since the angles and momenta of all particles were measured we had a 4-constraint fit. These constraints strongly discriminated against any events other than pion-proton elastic scattering.

The other type of background consisted of particles in the incident beam incorrectly labeled as π^- mesons. As was mentioned in Sec. 2B, we easily discriminated against K mesons and antiprotons with the threshold Čerenkov counter. However, the C counter was not able to discriminate against μ mesons and electrons.

The electron contamination in the beam was studied by running a Čerenkov pressure curve down to zero psi of ethane. This showed that electrons comprised less than 1% of the beam.

To study the μ-meson contamination, a 30-in.-long brass block was inserted in the beam. This was long enough to stop essentially all the pions, which interact strongly, but not sufficiently long to stop the μ mesons which interact only electromagnetically. The following fraction of the beam passed thru the brass: 6.8% at 5.2 GeV/c, 6.1% at 3.6 GeV/c, and 4.9% at 2.6 GeV/c. Unfortunately, this measurement was difficult to do accurately because of Coulomb scattering of the muons which depended on the beam angular divergence. Some of the pions, which interacted strongly, scattered forward and were counted as muons. At higher energies, fewer pions decayed but they decayed into a smaller forward cone. These effects work against each other but are difficult to calculate accurately. We concluded that the μ mesons comprised $(6\pm2)\%$ of the beam for all energies.

3. RESULTS

A. Corrections and Experimental Errors

There were two significant corrections to the raw data. The first correction was for the possible loss of either the scattered pion or proton due to a nuclear interaction before reaching the final scintillation counter. The proton had a 4% chance of interacting in the remainder of the hydrogen target, a 2.5% chance of interacting in the air, and a 5% chance of interacting in the early scintillators. Similarly, the scattered pion had a 4% probability of interacting in the target, a 1% chance in the air, and a 2.5% chance in the π_2 scintillator. The only uncertainty came from the fact that a nuclear interaction often gave a fast forward charged particle, which may have still triggered the last scintillation counter. The probability of this happening was estimated for each different region. When this was taken into account, the total correction to the raw data was 1.125. There was a $\pm2.5\%$ uncertainty in this number which appeared only as a normalization uncertainty because the spectrometers changed so little throughout the experiment.

The other significant correction was for the decay of the scattered pion before reaching the π_3 counter. The pion is unstable decaying into a muon and a neutrino with a mean life of 25.5 nsec in its rest frame. Approximately 25% of the backward scattered pions decayed before reaching the final counter in the pion telescope. However, the muons were emitted in a narrow forward cone with a maximum half-angle varying between 6.4° at 1.6 GeV/c incident beam momentum and 5.4° at 5.3 GeV/c. The backward-scattered pion momentum varied very little throughout the experiment; at an

incident beam momentum of 1.6 GeV/c, the momentum of the scattered pion was 0.35 GeV/c; at 5.3 GeV/c it was 0.42 GeV/c. Thus the coincidence was completed in many cases by the muons. Some lost events were also compensated for by muons from the decay of pions which would otherwise have missed the counters.

We assumed that all those backscattered pions which decayed in the first 80 in. before the π magnet were lost; that is, their muon was not counted. We also assumed that the pions which decayed in the remainder of the path were counted via their muon or by a compensating muon coming into the telescope. Since the momentum of the scattered pions did not vary much, this correction was essentially constant throughout the experiment. With these assumptions the correction for the decay of the scattered pions was 1.09 with an uncertainty of $\pm 5\%$.

Admittedly this is a somewhat rough calculation. To do it more accurately would require a complicated Monte Carlo program. This would require knowledge of the beam divergence and momentum spread, which was not known in great detail. Since the correction was small, the above calculation was sufficient.

Another possible correction was for the decay of some of the incident beam pions between B_3 and the liquid hydrogen target. However, this distance was only a few in. so this correction was well below 1%.

As the incident pion beam passed through the target, pions were removed by interaction with the target protons. Thus fewer pions were available to interact at the downstream end of the target than at the upstream end. This effect gave an over-all reduction in the effective beam intensity of 1%.

As was mentioned in Sec. 2, we were able to set 1% upper limits on both inelastic and accidental contamination.

A $(2\pm 1)\%$ subtraction was made for event originating in the hydrogen of the polystyrene in the B_2 and B_3 beam counters, since the system detected these elastic scattering events. In fact these events can be seen as the high channel events on the PHA time-of-flight spectrum (Fig. 6). Their high channel number and thus their relative time-of-flight difference (pion early, proton late) as well as their relative number corresponded to the expected event rate from these two beam counters.

More beam particles than were counted hit the H_2 target. If during the 2.5-nsec pulse width of the logic electronics, two or more beam pions passed through the beam counters, only one was counted while all of them hit the H_2 target. Each could interact and produce an event, which would be counted by the activated coincidence electronics as a good event.

We were not concerned about beam pions which passed through the beam counters during any dead time of the beam counters or the beam logic circuits. Since the beam telescope was in coincidence with the π and p telescopes, a beam coincidence was needed in order to count an event. So those beam particles, which arrived at any time other than the 2.5 nsec while the coincidence circuitry was activated, were excluded from the cross-section measurement.

The probability of two particles separated in time by less than 2.5 nsec both interacting to give events was extremely small. Therefore, to a very high degree of accuracy only the number of beam particles impinging on the hydrogen target needed to be modified. During acceleration the protons in the ZGS were grouped into rf bunches 8 nsec wide and 80 nsec apart. This resulted in an effective beam spill time a factor of 10 shorter than the observed time of 150 msec. Assuming negligible magnet ripple, the effective beam spill was 15 msec. Recalling that the beam intensity was 2×10^5 pions per pulse and that the live time was 2.5 nsec, it follows that the measured number BC was too small by 2%. This meant that the measured event rate should be multiplied by a factor 0.98 with an uncertainty of $\pm 1\%$.

Combining all these corrections and errors we obtained a net correction to the raw data of 1.25 with an error of $\pm 12\%$. This systematic error appeared primarily as a normalization error and could only result in all data points being shifted up or down together. We believe there was essentially no point-to-point systematic error. However, about $\pm 3\%$ of the systematic error may have a long-range energy dependence and thus all the high-energy points could be shifted by $\pm 3\%$ relative to the low-energy points.

The statistical errors were mostly between 10 and 15%. The uncertainty in the incident beam momentum was about ± 30 MeV/c. The angle subtended by the detection system corresponded to about 1° in the center-of-mass system.

B. Calculation of Cross Section

The differential cross section in the center-of-mass system was calculated from the formula

$$\frac{d\sigma}{d\Omega}=\frac{\text{No. events}}{(BC)N_0\rho t\Delta\Omega/A}. \tag{2}$$

The quantity BC was the measured number of beam pions, while N_0 was Avogadro's number, equal to 6.02×10^{23}. The density of liquid hydrogen ρ was taken to be 0.071, and the length of the target t was 30.5 cm; while A, the atomic weight of hydrogen was 1.01. The solid angle, $\Delta\Omega$, varied between 0.5 and 1.5 msr. The raw number of events was modified by the factor 1.25 as mentioned in Sec. 3A.

The center-of-mass differential cross section for $\pi^- p$ elastic scattering at 180° is plotted in Fig. 7 as a function of incident beam momentum. Only the statistical errors are shown; we believe that the systematic error of $\pm 12\%$ appears only as a normalization error. The data are also tabulated in Table I.

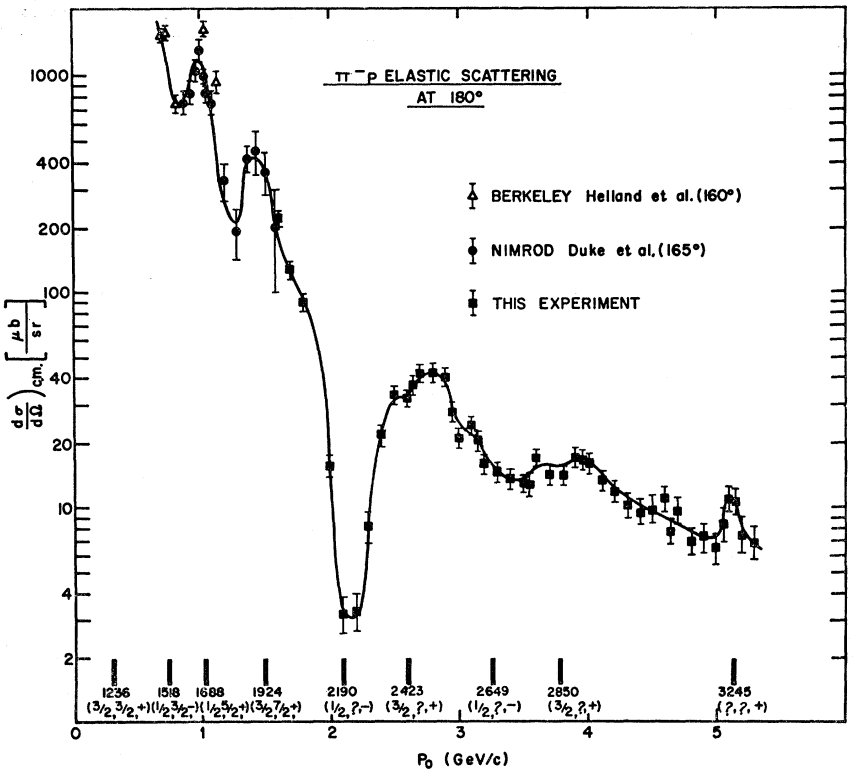

FIG. 7. Plot of $d\sigma/d\Omega$ against P_0, the incident π laboratory momentum, for $\pi^- p$ elastic scattering at 180°. The positions and properties of the N^* resonances are shown. The line drawn is a freehand fit to the data. The error bars shown are statistical. There is also a 12% normalization uncertainty. The mass (isospin, spin, and parity) of each resonance is given.

The line is a freehand fit to the data. The positions of all the known N^* resonances are shown. Given below them are their masses in MeV and their quantum numbers: isospin, spin, and parity. Data of other groups[3–9] who have measured $\pi^- p$ elastic scattering between 160° and 180° are also shown. Although most of these data are not at exactly 180° they are in qualitative agreement with our data.

4. DISCUSSION

The cross section plotted in Fig. 7 has considerable structure.[1,11] We believe that this structure is due to the existence of various N^* resonances. In elastic scattering each resonance appears as an intermediate state in the process

$$\pi^- + p \rightarrow N^* \rightarrow \pi^- + p. \quad (3)$$

In this type of process there are effects due to two types of amplitudes: the resonance amplitude and a nonresonant or background amplitude. These two amplitudes may interfere constructively, destructively, or not at all. There is a dramatic destructive interference at $P_0 = 2.15$ GeV/c which is quite interesting as the cross section drops almost two orders of magnitude in this region.

Another interesting result of the experiment is the large narrow peak in the cross section $P_0 = 5.12$ GeV/c. We believe that this is strong evidence for the existence of a nucleon resonance with a mass of 3245±10 MeV. This $N^*(3245)$ has a full width at half-maximum of less than 35 MeV and rises about 4 μb/sr above the nonresonant cross section. The width of the resonance is about 1% of its mass. This means that the particle is quite stable in spite of its large mass; its half-life is about 10^{-22} sec. It is very strange that such a heavy particle should be so stable. The only explanation of this fact proposed so far is that the $N^*(3245)$ has a very high spin ($\geq 21/2$) and is thus prohibited from decaying into lower states by the angular momentum barrier. The properties of the $N^*(3245)$ seem sufficiently strange that it is worth studying this resonance in some other process. There is a suggestion of a bump in the πp total cross section[12] at a mass of about 3220 MeV. However, the bump is just barely larger than the errors and is considerably broader than the peak we see. Such

[11] Alikhanov *et al.* studied $\pi^- n$ elastic scattering at 170° and saw a suggestion of structure: A. I. Alikhanov, G. L. Bayatyan, E. V. Brakhman, Yu. V. Galaktionov, G. P. Eliseev, F. A. Ech, O. Ya. Zel'dovich, L. G. Landsbert, V. A. Lyubimov, and I. V. Sidorov, JETP Pis'ma v Redaktsiyu **2**, 90 (1965) [English transl.: JETP Letters **2**, 57 (1965)]; Phys. Letters **19**, 345 (1965). Vovenko *et al.* saw no structure in $\pi^+ p$ elastic scattering at 180°: A. S. Vovenko, B. N. Gus'kov, M. F. Likhachev, A. L. Lyubimov, Yu. A. Matulenko, I. A. Savin, and V. S. Stavinskii, JETP Pis'ma v Redaktsiyu **2**, 409 (1965) [English transl.: JETP Letters **2**, 255 (1965)].

[12] A. Citron, W. Galbraith, T. F. Kycia, B. A. Leontic, R. H. Phillips, and A. Rousset, Phys. Rev. Letters **13**, 205 (1964). See this paper for earlier references. A. N. Diddens, E. W. Jenkins, T. F. Kycia, and D. F. Riley, *ibid.* **10**, 262 (1963); A. Citron, W. Galbraith, T. F. Kycia, B. A. Leontic, R. H. Phillips, and A. Rousset, *ibid.* **13**, 205 (1964).

a small broad bump is more or less consistent with the elasticity we observe, and the resolution of the total-cross-section experiment.

A. Parity

It is possible to determine the parity of each N^* resonance by observing whether the resonance causes destructive or constructive interference with the background amplitude. This idea has recently been advocated by Heinz and Ross[13] and others.[14,15]

There are two amplitudes for $\pi^- p$ elastic scattering: the resonant amplitude and the nonresonant or background amplitude. The resonant amplitude is the amplitude for elastic scattering via the channel

$$\pi^- + p \rightarrow N^* \rightarrow \pi^- + p. \tag{4}$$

There is no need to know its specific form at this time except that its sign is proportional to the parity of the N^*. The nonresonant or background amplitude is the amplitude for elastic scattering through all other channels. There have been several models for this amplitude. Heinz and Ross[13] suggested that it was due to baryon exchange. In many recent papers, Barger and Cline[16–19] have suggested that it is due to the exchange of a baryon Regge pole. There is no need to know its properties in detail to determine the parities of the nucleon isobars. One must only assume that it does not change sign as a function of energy.

Given that the nonresonant amplitude does not change sign as a function of energy, its sign can be determined by observing that the $N^*(1688)$ and $N^*(1924)$ both interfere constructively and are known[20] to have positive (+) parities. This implies that positive parities interfere constructively and negative parities interfere destructively. Thus we obtain the following parity assignments for the higher nucleon resonances: $N^*(2190)$, −; $N^*(2420)$, +; $N^*(2650)$, −; $N^*(2820)$, +; and $N^*(3245)$, +. In a recent $\pi^+ p$ elastic scattering experiment near 180°,[21] the $N^*(2420)$ and $N^*(2820)$ were confirmed to have positive (+) parity. In a recent $\pi^- p$ polarization experiment,[22] the $N^*(2190)$ was found to have negative (−) parity.

TABLE I. Center-of-mass cross sections for $\pi^- p$ elastic scattering at 180°.

P_0[a] (GeV/c)	S (GeV)^2	$d\sigma/d\Omega$ (μb/sr)	$d\sigma/dt$ μb/(GeV/c)^2	Error[b] (%)
1.60	3.91	220	1200	7
1.70	4.10	127	643	10
1.80	4.29	89.8	424	10
2.00	4.66	15.5	64.5	12
2.10	4.85	3.15	12.4	23
2.20	5.04	3.29	12.2	23
2.30	5.22	8.04	28.3	18
2.40	5.41	21.6	72.4	11
2.50	5.60	33.3	106	9
2.60	5.79	31.9	97.4	10
2.65	5.89	36.9	110	11
2.70	5.98	41.3	121	10
2.80	6.16	42.1	118	11
2.90	6.35	40.1	108	11
2.95	6.45	27.5	72.7	12
3.00	6.54	20.8	53.9	11
3.10	6.73	23.7	59.2	10
3.15	6.82	20.1	49.3	12
3.20	6.91	15.9	38.3	11
3.30	7.10	14.5	33.7	12
3.40	7.29	13.5	30.4	12
3.50	7.48	13.0	28.3	9
3.55	7.57	12.6	27.0	15
3.60	7.66	16.9	35.6	10
3.70	7.85	14.2	29.1	11
3.80	8.04	14.0	27.8	12
3.90	8.23	16.9	32.6	12
3.95	8.32	16.6	31.6	12
4.00	8.41	16.0	30.0	12
4.10	8.60	13.2	24.1	12
4.20	8.79	11.9	21.1	13
4.30	8.98	10.1	17.5	14
4.40	9.16	9.44	15.9	15
4.50	9.35	9.60	15.8	16
4.60	9.54	10.7	17.2	15
4.65	9.63	7.58	12.0	12
4.70	9.73	9.50	14.9	15
4.80	9.91	6.77	10.4	15
4.90	10.10	7.07	10.6	17
5.00	10.29	6.38	9.37	18
5.05	10.39	8.21	11.9	19
5.10	10.48	10.7	15.4	15
5.15	10.57	10.4	14.8	17
5.20	10.66	7.25	10.2	22
5.30	10.85	6.73	9.28	20

[a] The laboratory momentum P_0 is known to ± 0.03 GeV/c.
[b] The errors quoted are statistical, corresponding to one standard deviation. There is also a maximum normalization error of $\pm 12\%$.

B. Elasticity

If it is assumed that the nonresonant amplitude is a smooth function of energy, then we can determine the elasticities of various nucleon resonances by observing the size of each bump or valley in the 180° differential cross section. The elasticity is defined as the probability that a resonance will decay into the elastic channel

$$\chi = \Gamma_{el}/\Gamma_{tot}. \tag{5}$$

A useful expression[13–15] for the resonant amplitude is

$$f_R(E) = \lambda\!\!\!^{-}(E) C \chi (J+\tfrac{1}{2}) P \frac{\tfrac{1}{2}\Gamma}{M - E - \tfrac{1}{2} i\Gamma}. \tag{6}$$

The quantity $\lambda\!\!\!^{-}(E)$ is $\hbar/P_{c.m.}$, while C is the Clebsch-

[13] R. M. Heinz and M. H. Ross, Phys. Rev. Letters **14**, 1091 (1965); and (private communication).
[14] B. Jacobsohn and C. N. Yang (private communication).
[15] W. Layson, Nuovo Cimento **27**, 724 (1963); J. D. Jackson, *ibid.* **34**, 1644 (1964).
[16] V. Barger and D. Cline, Phys. Rev. Letters **16**, 913 (1966).
[17] V. Barger and D. Cline, in *Proceedings of the Thirteenth Annual International Conference on High-Energy Physics, Berkeley, 1966* (University of California Press, Berkeley, California, 1967).
[18] V. Barger and D. Cline, Phys. Letters **22**, 666 (1966).
[19] V. Barger and D. Cline, Phys. Rev. **155**, 1792 (1967).
[20] A. H. Rosenfeld, A. Barbaro-Galtieri, W. H. Barkas, P. L. Bastien, J. Kirz, and M. Roos, Rev. Mod. Phys. **37**, 663 (1965).
[21] T. Dobrowolski, B. N. Gus'kov, M. F. Likhachev, A. L. Lubimov, Yu. A. Matulenko, V. S. Stavinsky, and A. S. Vovenko, Phys. Letters **24B**, 203 (1967).
[22] A. Yokosawa, S. Suwa, R. E. Hill, R. J. Esterling, and N. E. Booth, Phys. Rev. Letters **16**, 714 (1966).

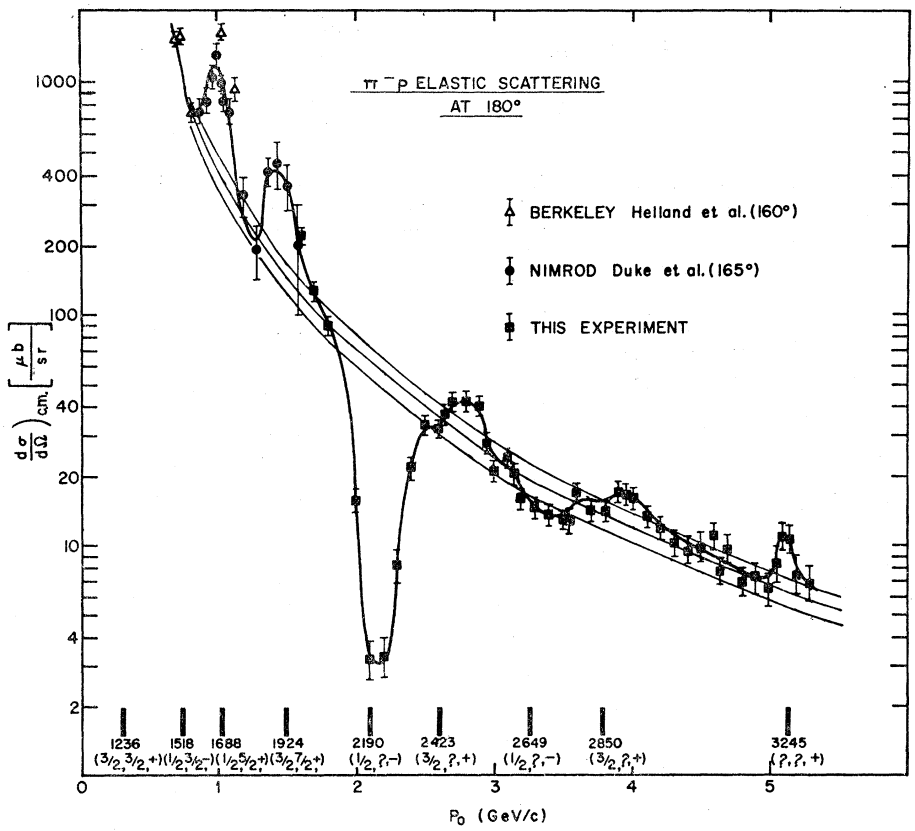

FIG. 8. Plot of $d\sigma/d\Omega$ against P_0 as in Fig. 7. We have also drawn the power-law fit to the background amplitude and the ±15% band.

Gordan coefficient given by

$$C=\tfrac{1}{3},\quad I=\tfrac{3}{2},$$
$$C=\tfrac{2}{3},\quad I=\tfrac{1}{2}. \tag{7}$$

The elasticity of the resonance is denoted by χ, while J is the spin and P is the parity. The mass and width of the resonance are denoted by M and Γ. The quantity E is the total center-of-mass energy of the system.

The background or nonresonant cross section was obtained from a straight-line fit to the data on a log-log plot. We found that the data fit the formula

$$(d\sigma/d\Omega)_b=A(P_0)^x, \tag{8}$$

where P_0 is the laboratory momentum of the incident pion. The two constants obtained from the best fit are

$$x=-2.58,$$
$$A=420(\mu\text{b/sr})(\text{GeV}/c)^{-x}. \tag{9}$$

This background cross section is plotted in Fig. 8 along with the data. We have also plotted a band which goes from 15% above Eq. (8) to 15% below. It is assumed that the true background cross section lies in this band.

Now we define R and I to be the real and imaginary parts of the background amplitudes:

$$R=\text{Re}(f_b),$$
$$I=\text{Im}(f_b), \tag{10}$$

where $(d\sigma/d\Omega)_b=|f_b|^2$. Then the cross section can be written as

$$d\sigma/d\Omega=[R+\text{Re}(f_R)]^2+[I+\text{Im}(f_R)]^2. \tag{11}$$

The resonant amplitude f_R is given by Eq. (6) and if we define the quantities

$$x\equiv M-E,$$
$$\gamma\equiv\tfrac{1}{2}\Gamma,$$
$$\alpha\equiv\frac{C[J+\frac{1}{2}]P\hbar\Gamma_{\text{el}}}{2P_{\text{c.m.}}}, \tag{12}$$

then we can express the cross section as

$$\frac{d\sigma}{d\Omega}=\left[R+\frac{\alpha x}{x^2+\gamma^2}\right]^2+\left[I+\frac{\alpha\gamma}{x^2+\gamma^2}\right]^2. \tag{13}$$

We can find the position of each maximum or minimum, x_0, by differentiating $d\sigma/d\Omega$ with respect to x and setting the derivative equal to zero:

$$\frac{d}{dx}\left(\frac{d\sigma}{d\Omega}\right)\bigg|_{x=x_0}=0. \tag{14}$$

This leads to the equation

$$R(\gamma^2-x_0^2)-2\gamma x_0 I-\alpha x_0=0. \tag{15}$$

TABLE II. Input parameters for Eq. (17). Also listed are the values of α and the parameters necessary to go from α to $\chi(J+\frac{1}{2})$ via Eq. (12). The values of $\chi(J+\frac{1}{2})$ appear in the last column. There is a factor of two uncertainty in these elasticities.

Resonance	$(d\sigma/d\Omega)_b$ (μb/sr)	$(d\sigma/d\Omega)_0$ (μb/sr)	Γ (MeV)	x_0 (MeV)	α^2/γ^2 (μb/sr)	C	$P_{\text{c.m.}}$ (GeV/c)	$\chi(J+\frac{1}{2})$
$N^*(2190)$	60	2.5	200	−33	42.9	$\frac{2}{3}$	0.91	0.45
$N^*(2420)$	28	42	280	−62	4.9	$\frac{1}{3}$	1.06	0.36
$N^*(2650)$	19	14	300	−32	0.43	$\frac{2}{3}$	1.17	0.06
$N^*(2850)$	12.5	17	300	−18	0.24	$\frac{1}{3}$	1.28	0.10
$N^*(3245)$	6.3	11	30	0	2.7	$\frac{1}{3}$?	1.48	0.37

This equation along with Eq. (13) and the fact that

$$\left(\frac{d\sigma}{d\Omega}\right)_b = R^2+I^2 \tag{16}$$

gives us a set of equations that we can solve for α, which is a measure of the elasticity for each resonance. In fact we find that α^2/γ^2 is given by the equation

$$\frac{\alpha^2}{\gamma^2} = (\sigma_0+\sigma_b)+\frac{x_0^2}{\gamma^2}(\sigma_b-\sigma_0) - 2\left[\sigma_0\left(\sigma_b+\frac{x_0^2}{\gamma^2}(\sigma_b-\sigma_0)\right)\right]^{1/2}. \tag{17}$$

We have used the notation

$$\sigma_0 = (d\sigma/d\Omega)_{x=x_0},$$
$$\sigma_b = (d\sigma/d\Omega)_b. \tag{18}$$

All the parameters that appear in Eq. (17) are obtainable from experimental data. We obtain the value of σ_b from Eq. (8) which gives a good fit to our data. The positions of the minimum or maximum x_0 and the value of σ_0 at this point are taken from Fig. 8. The values of $\gamma=\frac{1}{2}\Gamma$ are taken from total-cross-section measurements except for the $N^*(3245)$ where we assign the value $\Gamma=30$ MeV. All these input parameters appear in Table II.

The calculated value of α^2/γ^2 also appears in Table II. The corresponding values of $\chi(J+\frac{1}{2})$ appear in the last column of Table II. These values of the elasticity differ significantly from the values proposed by others[16–19] on the basis of this experiment and total-cross-section measurements.[12]

We believe that there is an uncertainty of about a factor of two in our quoted values of elasticities. This arises primarily from the uncertainty in the background cross section σ_b. However we also believe that these values are more reliable than other values which have been obtained from our data, by employing a specific Regge-pole model.[16–19] It also appears to us that this fixed-angle differential cross section depends more sensitively on the elasticity than does the total cross section.

In conclusion, it is felt that the values of $\chi(J+\frac{1}{2})$ given in Table II are the most reliable values presently available even though they have a factor of two uncertainty.

ACKNOWLEDGMENTS

We are especially grateful to Professor M. H. Ross for his many suggestions in the early stages of the experiment. We would also like to thank Professor C. T. Coffin, Professor L. W. Jones, Professor G. L. Kane, Professor D. I. Meyer, Professor O. E. Overseth, and Professor C. N. Yang for their comments. We thank Dr. N. Stanton, H. Rosdolsky, and R. Mead for their help in running the experiment. We are very grateful to the entire ZGS staff for their invaluable support and encouragement throughout the experiment. One of us (A. D. K.) would like to acknowledge the hospitality of the Aspen Institute Physics Division during the final stages of writing this paper.